PHYSICAL REVIEW B **96**, 100401(R) (2017)

Excitation and tailoring of diffractive spin-wave beams in NiFe using nonuniform microwave antennas

H. S. Körner, J. Stigloher, and C. H. Back*

Institut für Experimentelle und Angewandte Physik, Universität Regensburg, D-93040 Regensburg, Germany

(Received 6 April 2017; revised manuscript received 30 May 2017; published 5 September 2017)

We experimentally demonstrate by time-resolved scanning magneto-optical Kerr microscopy the possibility to locally excite multiple spin-wave beams in the dipolar-dominated regime in metallic NiFe films. For this purpose we employ differently shaped nonuniform microwave antennas consisting of several coplanar waveguide sections different in size, thereby adapting an approach for the generation of spin-wave beams in the exchange-dominated regime suggested by Gruszecki *et al.* [Sci. Rep. **6**, 22367 (2016)]. The occurring spin-wave beams are diffractive and we show that the width of the beam and its widening as it propagates can be tailored by the shape and the length of the nonuniformity. Moreover, the propagation direction of the diffractive beams can be manipulated by changing the bias field direction.

DOI: 10.1103/PhysRevB.96.100401

At the heart of the field of magnonics is the design of devices and logic circuits that are based on the elementary excitations of ordered magnetic materials: spin-waves (SWs) or their quanta, magnons [1]. Here, magnons are used to process and transport information. Within the field of magnonics [2–8], the implementation of concepts originating from optics has become an active field of research. Here, the aim is to achieve maximum flexibility concerning manipulation such as steering of SWs with the ability to reduce the required footprint of a device while maintaining high-frequency operation [1]. So-called SW nano-optics [9] require the generation and manipulation of SW beams in the microwave frequency range and enable the realization of devices like SW fibers [10,11] or the exploitation of refraction and reflection effects [12–14]. Within the last few years, various approaches to generate SW beams were proposed and investigated.

(i) Caustic SW beams occur in anisotropic media since here the group velocity $\vec{v}_{gr} = 2\pi\,\partial f/\partial\vec{k}$ indicating the direction of the energy propagation does not, in general, coincide with the direction of the wave vector $\vec{k}$. Consequently, when the anisotropy is sufficiently strong, the direction of the group velocity of the SW beam may become independent of the wave vectors forming the beam in the vicinity of a certain carrier wave vector. Hence, wave packets excited with a broad angular spectrum of wave vectors may be channeled along this direction. SW caustics present quasinondiffractive beams as they maintain their transverse aperture over large propagation distances (on the order of several millimeters) [15]. Experimentally the creation and occurrence of these type of SW beams was observed when SWs propagate from a microwaveguide into a continuous film [15,16], being emitted from edge modes [17], or when using single antidots [18] while unidirectional SW caustics were recently examined theoretically in ultrathin ferromagnets with Dzyloshinskii-Moriya interaction [19,20].

(ii) SW propagation in antidot lattices [21,22] and the efficient SW propagation occurring in confined narrow channels [23,24] can also be regarded as a kind of SW beam thus representing possible other mechanisms to generate SW beams.

(iii) Moreover, Gruszecki *et al.* presented another approach enabling the generation of multiple narrow SW beams in the exchange-dominated regime [25] in magnetic full films. Here, the desired beam type behavior can be achieved with the aid of a properly designed coplanar waveguide (CPW) generating a nonuniform magnetic microwave field [26]. However, there are two crucial constraints. First, the exchange-dominated regime cannot be accessed by magneto-optical techniques such as time-resolved scanning magneto-optical Kerr microscopy (TRMOKE) or Brillouin light scattering since the corresponding SW wavelengths are below the optical detection limit. Secondly, the dimensions of the constituents of microwave antennas enabling the generation of SWs belonging to this regime need to be on the order of about 100 nm which is at the edge of feasibility using current common state-of-the-art nanofabrication techniques.

In this Rapid Communication, we experimentally demonstrate by TRMOKE the possibility to excite SW beams in the dipolar-dominated regime in thin metallic NiFe films. For this purpose we adapted the approach suggested by Gruszecki *et al.* [26] and fabricated nonuniform microwave antennas consisting of differently sized CPW segments thereby having different excitation spectra. In contrast to SW caustics observed in micrometer-thick yttrium iron garnet (YIG) films [15], here, all occurring SW beams are diffractive. Their propagation distance is inherently limited by the attenuation length which is only on the order of several micrometers. We also show that the spatial structure of the propagating beams can be tailored by both the shape and the length of the nonuniformity. Moreover, the propagation direction of the diffractive beams can be manipulated by changing the direction of the in-plane (IP) bias field.

The study was performed in the Damon-Eshbach (DE) geometry [25]. Here, SWs with wave vector $\vec{k}$ excited by the nonuniform microwave antenna propagate along the x direction while the external magnetic bias field $\vec{H}_0$ is applied along the z direction as illustrated in Fig. 1(a). The generation of SW beams was investigated in NiFe ($Ni_{80}Fe_{20}$) films grown by thermal evaporation on a GaAs substrate. In contrast to YIG, in metallic films, the attenuation length L_{att} of DE SWs

*christian.back@physik.uni-regensburg.de

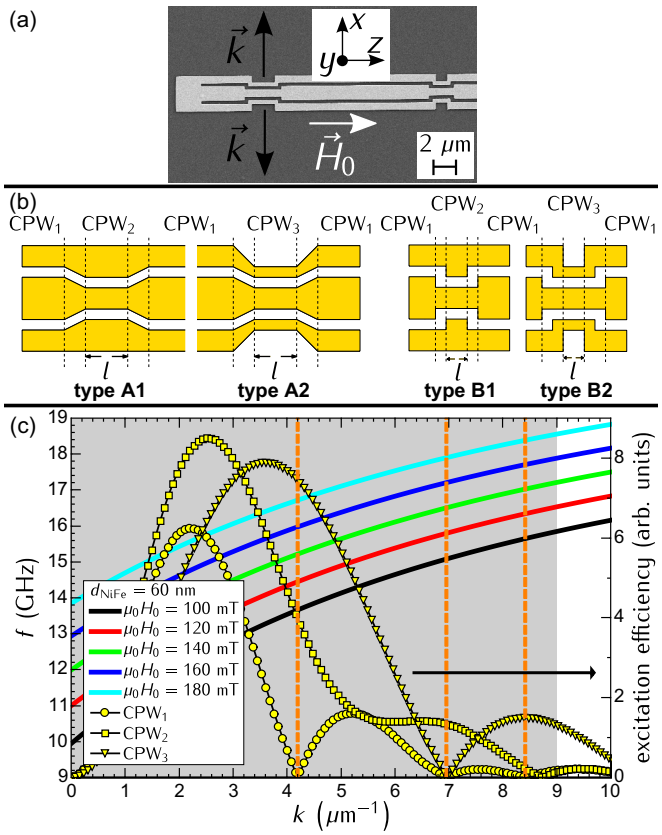

FIG. 1. (a) Scanning electron microscopy image of one sample illustrating the experimental geometry. SWs/SW beams with wave vector $\vec{k}$ excited by the nonuniform microwave antenna propagate along the x direction on either side of the antenna while the external magnetic field $\vec{H}_0$ is applied along the z direction. (b) Schematics of the four different types of nonuniform microwave antenna fabricated. Types A1/B1 (A2/B2) are composed of several CPW_1 and CPW_2 (CPW_1 and CPW_3) segments. Type A (type B) antennas have slanted (sharp edged) transitions between neighboring segments. The length l of the individual CPW_2 (CPW_3) sections can be varied [cf. (a)]. (c) Calculated excitation spectra of the individual CPW segments (CPW_{1-3}) along with DE SW dispersion curves for different H_0 in the case of a 60-nm-thick NiFe film. The gray-shaded area denotes the wave number range accessible by TRMOKE. The dashed orange lines indicate distinct wave numbers $\tilde{k}$ which cannot be excited by the CPW_1 segment, but by either of the other two. Any intercept of these lines with the dispersion curves denotes a pair of values $(\tilde{f}, \tilde{H}_0)$ for which SW beams with wave number $\tilde{k}$ are expected to occur.

is much smaller due to a much larger magnetic damping. Hence, in order to be able to observe the propagation of SW beams over large distances, we took advantage of the fact that L_{att} scales linearly with the film thickness d and chose $d_{NiFe} = 50$–60 nm resulting in L_{att} values being on the order of several micrometers. On top of the magnetic film, differently shaped nonuniform microwave antennas in the shape of shorted CPWs were patterned by electron beam lithography and subsequent thermal evaporation of Cr(10 nm)/Au(80–100 nm). They were electrically decoupled from the metallic NiFe film by an 80-nm-thick insulating Al_2O_3 layer grown by atomic layer deposition. The smallest feature size possible was given by the fabrication process.

In general, a microwave antenna excites a broad range of wave vectors [27]. The shape of the excitation spectrum indicating how efficiently each wave number can be excited (i.e., nonvanishing excitation efficiency) or not excited at all (i.e., vanishing excitation efficiency) is inherently determined by the antenna dimensions. It is given by the Fourier transform of the spatial profiles of the dynamic IP and out-of-plane (OOP) microwave fields generated by the microwave antenna which can be calculated using the two-dimensional Biot-Savart law assuming a uniform current density within the CPW. They are identical in the studied wave number range. For the generation of locally excited SW beams propagating in unpatterned films using nonuniform microwave antennas it is mandatory that the excitation spectra of the individual CPW segments such an antenna is composed of are different. Here, we fabricated nonuniform antennas consisting of three different segments denoted as CPW_{1-3} as depicted in Fig. 1(b). The dimensions (nominal width in micrometers) of signal line, ground line, and gap were 1.2/0.6/0.3 (CPW_1), 0.6/0.9/0.3 (CPW_2), and 0.6/0.3/0.3 (CPW_3). The corresponding calculated excitation spectra are elucidated in Fig. 1(c). Here, the focus is on the zero points of the individual spectra. The dashed lines mark distinct wave numbers $\tilde{k}$ which cannot be excited by a CPW_1 segment, but by either a CPW_2 or a CPW_3 segment. Hence, in principle, using one nonuniform microwave antenna consisting of a series of CPW_1 and CPW_2/CPW_3 segments should enable the local excitation of multiple SW beams simultaneously. For any combination of excitation frequency f and H_0, the corresponding k is defined by the DE SW dispersion [25]. Several dispersion curves $f(k)$ are illustrated in Fig. 1(c) in the case of a 60-nm-thick NiFe film ($\gamma = 193 \times 10^9$ rad/(Ts), $\mu_0 M_S = 0.95$ T) for different H_0. Here, any intersection between the dashed lines and the dispersion curves denotes a certain set of values $(\tilde{f}, \tilde{H}_0)$ for which SW beams with wave number $\tilde{k}$ are expected to occur. Appropriate f are in the range from 12 to 18 GHz.

Moreover, the length l of the CPW_2 (CPW_3) section was also varied from 500 nm to 10 μm to check the possibility of tailoring the initial SW beam width, and the transitions between the CPW_1 and CPW_2 (CPW_3) segments were patterned both sharp edged (types B1 and B2) and slanted (types A1 and A2) as illustrated in Fig. 1(b) to study their effect on the SW beam characteristics as well.

In the NiFe film, SW dynamics was accessed magneto-optically by TRMOKE performed in the polar geometry, i.e., with sensitivity to the dynamic OOP component of the propagating SWs. The probing laser pulses trains had a wavelength of about 400 nm at a repetition rate of 80 MHz. For the time resolution, the phase ϕ between the laser pulses and the microwave excitation of the antenna was continuously locked, which was achieved by an active feedback loop. We note that here one is not interested in the absolute phase as long as it remains constant. Given by the optical detection limit of the microscope employed wave numbers up to approximately 9 μm^{-1} [14,28,29] could be detected as indicated by the gray-shaded area in Fig. 1(c).

The TRMOKE setup was operated in two modes providing complementary information. In the first mode, for fixed f, the position of the laser spot was kept at a fixed position on the sample (≈3–4 μm away from the antenna) while H_0 was

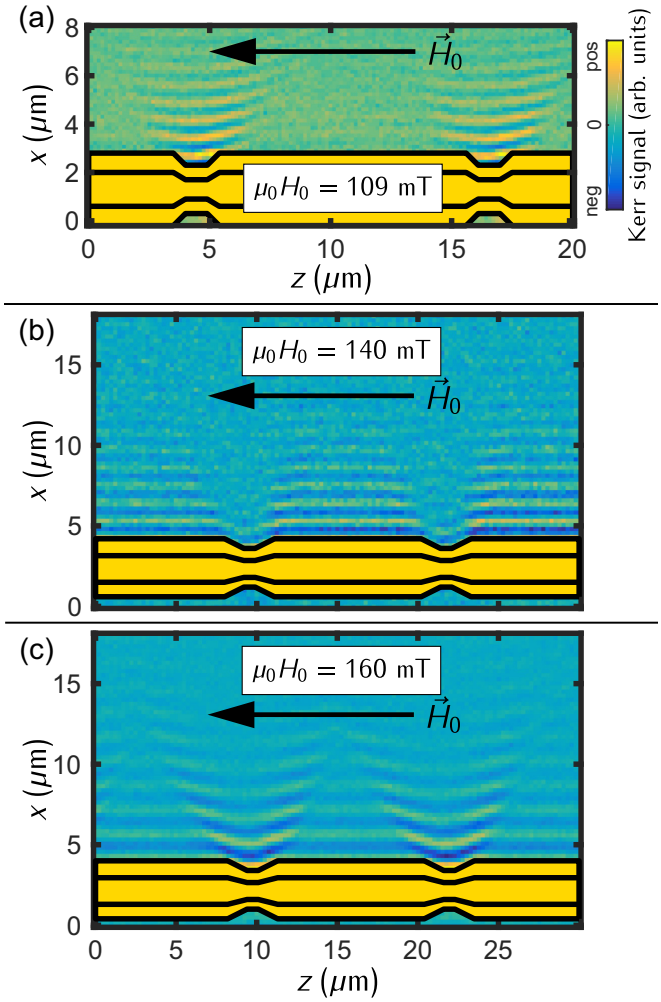

FIG. 2. Selection of Kerr images obtained at 16.08 GHz using a type A2 antenna (yellow). (a) Simultaneous excitation of two diffractive SW beams at 109 mT propagating above the two 1-μm-long CPW_3 segments. (b) Opposite situation as in (a) at 140 mT. Now, diffractive SW beams are excited by the CPW_1 sections. (c) At 160 mT, SWs are excited by all CPW segments. On top of that, one observes an enhanced SW amplitude along distinct directions.

swept. From the resulting SW resonance spectra recorded for $\phi = 0^\circ$ and 90° we determined the appropriate field range in which SW propagation could be detected at fixed f. Then, in the second mode, H_0 was fixed while the sample was scanned in the xz plane allowing us to directly image the excited SWs propagating on either side of the antenna. In the resulting Kerr images, the position of the nonuniform microwave antenna was extracted from the corresponding topography image of the sample which was acquired simultaneously and contained information about the local sample reflectivity. Due to the amplitude nonreciprocity inherently present when exciting SWs by CPWs [28,30,31] we focused on the side of the antenna where the SW amplitude was larger at a given field direction.

The experimental findings shown and discussed below were obtained at $f = 16.08$ GHz if not otherwise stated. First, we employed a type A2 antenna. Here, the simultaneous excitation of multiple SW beams by the CPW_3 segments was observed at 109 mT as depicted in Fig. 2(a). This field value was in reasonable agreement with the right dashed line in Fig. 1(c)

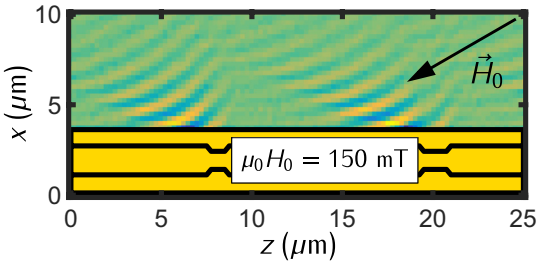

FIG. 3. Simultaneous excitation of two diffractive SW beams at 150 mT using a type A1 antenna. The IP direction of the bias field is rotated with respect to the z direction. Consequently, the propagation direction of the diffractive SW beams is rotated as well.

as one has to keep in mind that the excitation spectra were calculated for antennas with well-known dimensions, whereas the dimensions of the fabricated nonuniform microwave antennas could differ from the desired ones (up to 100 nm) resulting in slightly different shapes of the corresponding excitation spectra. The occurring SW beams were clearly diffractive. Their width increased from $\approx$4 μm right next to the antenna to about 7 μm for a propagation distance of about 5 μm. We note that in contrast to nondiffractive caustic SW beams for which there is a solid definition for the width of the beam [15], here, in the case of diffractive SW beams, we used this expression to describe the width of the beam wavefront at a certain distance away from the nonuniform microwave antenna. It quantified the width of the region in the Kerr images where still a finite SW amplitude could be detected. Moreover, note that the Kerr signal was rather weak since the excitation efficiency of the CPW_3 segment was low for wave numbers close to 8.5 μm^{-1}.

Then, H_0 was raised to 140 mT. Now, the situation was opposite. As clearly visible in Fig. 2(b), propagating SWs could not be excited by the CPW_3 segments, but only by the CPW_1 segments. Although the length of these segments was about 10 μm, i.e., much larger than the 1-μm-long CPW_3 segment, the excited propagating SWs could be regarded as much wider SW beams since they were separated by regions without any SW propagation. These wider beams were also diffractive. Here, however, their width decreased the further they propagated. This behavior was attributed to the slanted transitions between the neighboring CPW segments of the type A2 antenna. At 160 mT, propagating SWs were excited by the whole nonuniform microwave antenna. Moreover, as can be seen in Fig. 2(c), we observed an enhanced SW amplitude along distinct directions within the xz plane due to the superposition of SWs with different IP wave vectors $\vec{k}$. However, owing to the relatively short attenuation length in NiFe compared to thick YIG, we could not unambiguously clarify whether this feature is an interference effect or due to the onset of the formation of SW caustics which also might be possible since, at this bias field magnitude, the IP SW dispersion [14] reveals that the direction of the group velocity denoting the direction of energy flow becomes independent of the $\vec{k}$ direction.

Furthermore, only in the case of the type A antennas, we investigated if the propagation direction of the diffractive SW beams could be manipulated as well, thus enabling SW beam steering. As illustrated in Fig. 3, the propagation direction of two diffractive SW beams, in this case being excited by a type

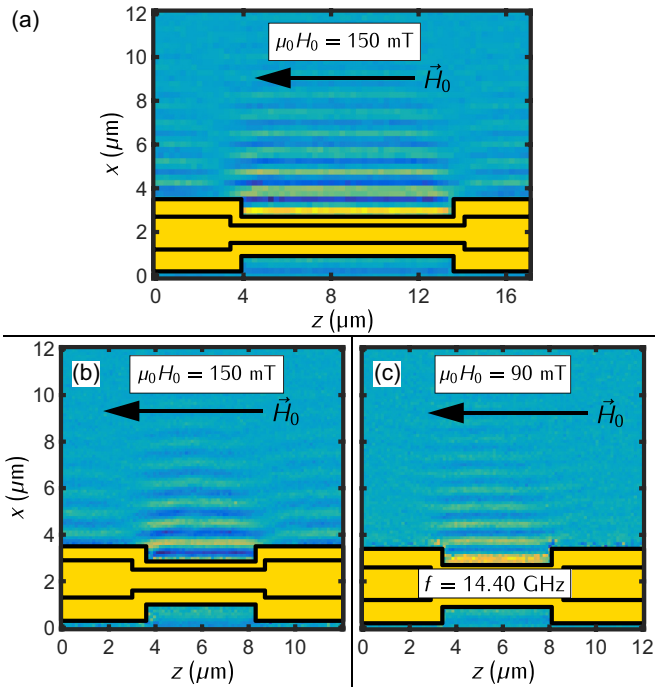

FIG. 4. Selection of Kerr images obtained using a type B2 antenna (yellow). (a) A diffractive SW beam is excited by a 10-μm-long CPW_3 segment. (b) Same situation as in (a) on top of a 5-μm-long CPW_3 segment. (c) Same situation as in (b), now at 14.40 GHz and 90 mT.

A1 antenna, was turned away from the x direction by rotating the direction of the IP bias field with respect to the z direction. The bias field strength was different compared to the situation shown in Fig. 2(a) since a different type A antenna was used. It is assumed that the slanted transitions facilitate the beam steering. To clarify whether it is actually affected by the shape of the transitions, further measurements would be required which would go beyond the scope of this work.

Next, we investigated if the diffractive behavior of the SW beam could be tailored by the shape of the nonuniformity of the antenna. For this purpose, we employed a type B2 antenna fabricated on top of another NiFe film (i.e., slightly different thickness and material parameters). Hence, the bias field values for the occurrence of SW beams and the corresponding wave numbers do not match with the dispersion curves shown in Fig. 1(c). At 150 mT, propagating SW beams were observed again, indicated by a significantly enhanced SW amplitude above the CPW_3 segment as illustrated in Fig. 4(a). Note that propagating SWs with a much smaller amplitude were also excited by the CPW_1 segments, but only because the bias field magnitude was not perfectly tuned to match the wave number for which the excitation efficiency of the CPW_1 segment vanished. Hence, it was finite, but very weak. However, more importantly, now, the beam width did not change considerably within the detectable propagation distance compared with the SW beams excited by the type A2 antenna. After $\approx$6 μm, it was almost the same as its initial width given by the length of the CPW_3 segment ($\approx$10 μm). The same characteristic occurred when the length of the CPW_3 was reduced to 5 μm as shown in Fig. 4(b). This behavior is attributed to the sharp edged transition between neighboring CPW elements of the type B2 (type B1) antenna. Here, each CPW element dominantly favors the excitation of DE SWs, i.e., SWs with the wave vector $\vec{k}$ being oriented perpendicular to the applied field direction $\vec{H}_0$. In contrast, the slanted transitions of the type A2 (type A1) antenna most likely also facilitate the excitation of wave components having different IP wave vectors. These findings reveal that the diffractive behavior of a SW beam excited in the dipolar-dominated regime depends crucially on the shape of the nonuniformities integrated into the microwave antenna and that the desired width of such a "diffraction tuned" SW beam can be tailored by the length of the exciting CPW segment. Finally, in order to prove that the frequency of the diffractive SW beams could be tuned as well, we set f to 14.40 GHz. In agreement with the DE SW dispersion, now, a lower bias field magnitude was required to observe the same SW beam characteristics as at 16.08 GHz as illustrated in Fig. 4(c). Note that, now, it matched the wave number very well for which the excitation efficiency of the CPW_1 segment vanished.

In summary, we have demonstrated that it is possible to generate multiple SW beams in the dipolar-dominated regime in metallic NiFe films simultaneously by using nonuniform microwave antennas being composed of several CPW segments with different dimensions. The excited SWs/SW beams were detected by TRMOKE. All occurring SW beams were diffractive, i.e., their width changed as they propagated. Moreover, we have shown that both the diffractive behavior and the width of the propagating SW beams could be tailored by the shape and length of the nonuniformity. The frequency of the SW beams could be tuned as well when the bias field magnitude was adjusted simultaneously. Moreover, in the case of slanted transitions between neighboring CPW segments, the propagation direction of the diffractive SW beams could be changed by rotating the IP bias field direction. These findings are interesting for the development of magnonic devices where the control, shaping and steering of SW beams becomes essential.

We gratefully acknowledge funding by the Deutsche Forschungsgemeinschaft via SFB 689.

[1] A. V. Chumak, V. I. Vasyuchka, A. A. Serga, and B. Hillebrands, Nat. Phys. **11**, 453 (2015).

[2] V. E. Demidov, S. O. Demokritov, K. Rott, P. Krzysteczko, and G. Reiss, Appl. Phys. Lett. **91**, 252504 (2007).

[3] K. Sekiguchi, K. Yamada, S. M. Seo, K. J. Lee, D. Chiba, K. Kobayashi, and T. Ono, Appl. Phys. Lett. **97**, 022508 (2010).

[4] A. V. Chumak, A. A. Serga, and B. Hillebrands, Nat. Commun. **5**, 4700 (2014).

[5] K. Vogt, F. Y. Fradin, J. E. Pearson, T. Sebastian, S. D. Bader, B. Hillebrands, A. Hoffmann, and H. Schultheiss, Nat. Commun. **5**, 3727 (2014).

[6] N. Sato, S.-J. Lee, S.-W. Lee, K.-J. Lee, and K. Sekiguchi, Appl. Phys. Express **9**, 083001 (2016).

[7] V. V. Kruglyak, S. O. Demokritov, and D. Grundler, J. Phys. D: Appl. Phys. **43**, 260301 (2010).
[8] P. Pirro, T. Koyama, T. Brächer, T. Sebastian, B. Leven, and B. Hillebrands, Appl. Phys. Lett. **106**, 232405 (2015).
[9] V. E. Demidov, S. O. Demokritov, K. Rott, P. Krzysteczko, and G. Reiss, Appl. Phys. Lett. **92**, 232503 (2008).
[10] X. Xing and Y. Zhou, NPG Asia Mater. **8**, e246 (2016).
[11] W. Yu, J. Lan, R. Wu, and J. Xiao, Phys. Rev. B **94**, 140410 (2016).
[12] P. Gruszecki, J. Romero-Vivas, Y. S. Dadoenkova, N. N. Dadoenkova, I. L. Lyubchanskii, and M. Krawczyk, Appl. Phys. Lett. **105**, 242406 (2014).
[13] P. Gruszecki, M. Mailyan, O. Gorobets, and M. Krawczyk, Phys. Rev. B **95**, 014421 (2017).
[14] J. Stigloher, M. Decker, H. S. Körner, K. Tanabe, T. Moriyama, T. Taniguchi, H. Hata, M. Madami, G. Gubbiotti, K. Kobayashi, T. Ono, and C. H. Back, Phys. Rev. Lett. **117**, 037204 (2016).
[15] T. Schneider, A. A. Serga, A. V. Chumak, C. W. Sandweg, S. Trudel, S. Wolff, M. P. Kostylev, V. S. Tiberkevich, A. N. Slavin, and B. Hillebrands, Phys. Rev. Lett. **104**, 197203 (2010).
[16] V. E. Demidov, S. O. Demokritov, D. Birt, B. O'Gorman, M. Tsoi, and X. Li, Phys. Rev. B **80**, 014429 (2009).
[17] T. Sebastian, T. Brächer, P. Pirro, A. A. Serga, B. Hillebrands, T. Kubota, H. Naganuma, M. Oogane, and Y. Ando, Phys. Rev. Lett. **110**, 067201 (2013).
[18] R. Gieniusz, H. Ulrichs, V. D. Bessonov, U. Guzowska, A. I. Stognii, and A. Maziewski, Appl. Phys. Lett. **102**, 102409 (2013).
[19] J.-V. Kim, R. L. Stamps, and R. E. Camley, Phys. Rev. Lett. **117**, 197204 (2016).
[20] T. Brächer, O. Boulle, G. Gaudin, and P. Pirro, Phys. Rev. B **95**, 064429 (2017).
[21] S. Neusser, G. Durr, H. G. Bauer, S. Tacchi, M. Madami, G. Woltersdorf, G. Gubbiotti, C. H. Back, and D. Grundler, Phys. Rev. Lett. **105**, 067208 (2010).
[22] S. Neusser, H. G. Bauer, G. Duerr, R. Huber, S. Mamica, G. Woltersdorf, M. Krawczyk, C. H. Back, and D. Grundler, Phys. Rev. B **84**, 184411 (2011).
[23] G. Duerr, K. Thurner, J. Topp, R. Huber, and D. Grundler, Phys. Rev. Lett. **108**, 227202 (2012).
[24] K. Wagner, A. Kákay, K. Schultheiss, A. Henschke, T. Sebastian, and H. Schultheiss, Nat. Nanotechnol. **11**, 432 (2016).
[25] D. D. Stancil and A. Prabhakar, *Spin Waves—Theory and Applications* (Springer US, New York, 2009).
[26] P. Gruszecki, M. Kasprzak, A. E. Serebryannikov, M. Krawczyk, and W. Śmigaj, Sci. Rep. **6**, 22367 (2016).
[27] H. Bauer, J.-Y. Chauleau, G. Woltersdorf, and C. Back, in *Ultrafast Magnetism I*, Springer Proceedings in Physics (Springer International Publishing, Cham, 2015), Vol. 159, pp. 83–85.
[28] J.-Y. Chauleau, H. G. Bauer, H. S. Körner, J. Stigloher, M. Härtinger, G. Woltersdorf, and C. H. Back, Phys. Rev. B **89**, 020403(R) (2014).
[29] H. S. Körner, J. Stigloher, H. G. Bauer, H. Hata, T. Taniguchi, T. Moriyama, T. Ono, and C. H. Back, Phys. Rev. B **92**, 220413(R) (2015).
[30] M. Bailleul, D. Olligs, and C. Fermon, Appl. Phys. Lett. **83**, 972 (2003).
[31] M. Jamali, J. H. Kwon, S.-M. Seo, K.-J. Lee, and H. Yang, Sci. Rep. **3**, 3160 (2013).